Efficient state transfer in an ultracold dense gas of heteronuclear molecules

S. OSPELKAUS[1], A. PE'ER[1], K.-K. NI[1], J. J. ZIRBEL[1], B. NEYENHUIS[1], S. KOTOCHIGOVA[2], P. S. JULIENNE[3], J. YE[1]* AND D. S. JIN[1]*

[1]JILA, National Institute of Standards and Technology and University of Colorado, Department of Physics, University of Colorado, Boulder, Colorado 80309-0440, USA
[2]Physics Department, Temple University, Philadelphia, Pennsylvania 19122-6082, USA
[3]Joint Quantum Institute, National Institute of Standards and Technology and University of Maryland, Gaithersburg, Maryland 20899-8423, USA
*e-mail: junye@jilau1.colorado.edu; jin@jilau1.colorado.edu

Published online: 22 June 2008; doi:10.1038/nphys997

Polar molecules have bright prospects for novel quantum gases with long-range and anisotropic interactions[1], and could find uses in quantum information science[2] and in precision measurements[3–5]. However, high-density clouds of ultracold polar molecules have so far not been produced. Here, we report a key step towards this goal. We start from an ultracold dense gas of loosely bound ^{40}K^{87}Rb Feshbach molecules[6,7] with typical binding energies of a few hundred kilohertz, and coherently transfer these molecules in a single transfer step into a vibrational level of the ground-state molecular potential bound by more than 10 GHz. Starting with a single initial state prepared with Feshbach association[8], we achieve a transfer efficiency of 84%. Given favourable Franck–Condon factors[9,10], the presented technique can be extended to access much more deeply bound vibrational levels and those exhibiting a significant dipole moment.

Strategies for the realization of an ultracold dense gas of polar molecules have generally followed two different approaches. The first is to directly cool ground-state polar molecules by means of buffer gas cooling[11], Stark deceleration[12,13] or velocity filtering[14]. However, direct cooling strategies have typically been restricted to the millikelvin temperature range. Photoassociation schemes[15], on the other hand, have the advantage of using high-density ultracold atomic clouds as a promising starting point. The combination of photoassociation and pump–dump schemes has recently resulted in the formation of ground-state polar molecules[9]. However, the realization of an ultracold dense gas of polar molecules has so far not been reported. Photoassociation schemes rely on spontaneous emission to populate bound molecular levels in the ground-state molecular potential[9,16]. The spontaneous processes result in a large spread of population among several continuum and bound molecular states. Two-colour photoassociation schemes suffer from the small wavefunction overlap between the continuum states of colliding atoms and the localized molecular states, resulting in the necessity of large optical power, which then opens up other loss channels[17,18]. This wavefunction overlap can be significantly enhanced by starting from a weakly bound molecule as compared with the continuum state of two colliding atoms. Weakly bound molecules in well-defined near-dissociation quantum states can be efficiently created using magnetic-field-tunable Feshbach resonances in ultracold atomic gases[8]. The resulting ensembles of Feshbach molecules constitute an excellent launching stage for the application of coherent optical transfer schemes to produce molecules in deeply bound vibrational levels. The combination of heteronuclear Feshbach molecule creation[6,7,19,20] with coherent de-excitation schemes[21] might therefore result in the creation of an ultracold dense gas of polar molecules.

In the homonuclear Rb_2 system, Feshbach molecules have been used as a starting point for coherent two-photon transfer into a state bound by $\sim h \times 500$ MHz (ref. 22). In addition, radiofrequency manipulation schemes have been used in the Rb_2 system, achieving binding energies of $> h \times 3$ GHz (ref. 23). These results represent a powerful demonstration of the degree of control available in ultracold gases. Here, we report on coherent transfer of heteronuclear Feshbach molecules into a more deeply bound vibrational level of the ground-state molecular potential (see Table 1). We thus demonstrate a key step towards the realization of a quantum degenerate ultracold gas of polar molecules. Using two phase-coherent laser fields to couple the initial Feshbach state $|i\rangle$ and the target state $|t\rangle$ to a common electronically excited state $|e\rangle$ (Fig. 1a), stimulated Raman adiabatic passage[24] (STIRAP) is used to coherently transfer the population of $|i\rangle$ to $|t\rangle$. Through this transfer process, we produce a dense ultracold cloud of heteronuclear molecules with a binding energy of $> h \times 10$ GHz. An essential prerequisite for the successful demonstration of STIRAP in this system has been careful one-photon spectroscopic investigation of the so-far unknown ^{40}K^{87}Rb excited-state molecular potential below the $4S_{1/2} + 5P_{1/2}$ threshold and precise two-photon spectroscopy of more deeply bound vibrational levels in the ground-state molecular potential of ^{40}K^{87}Rb.

Starting from a near-quantum-degenerate Bose–Fermi mixture of ^{87}Rb and ^{40}K atoms confined in a single-beam optical dipole trap, we use magnetic-field ramps across a Feshbach resonance at 546.7 G to create 2×10^4 heteronuclear Feshbach molecules with a density of $\approx 5 \times 10^{11}$ cm^{-3} (see the Methods section). At a magnetic field of $B = 545.88$ G, the Feshbach molecules have a binding energy of $h \times (270 \pm 50)$ kHz and can be directly, and selectively, imaged by high-field resonant absorption imaging (see the Methods section). The Feshbach molecules are in a superposition of the open channel $\mathrm{K}|F = 9/2, m_F = -9/2\rangle + \mathrm{Rb}|F = 1, m_F = 1\rangle$ and the adiabatically connecting closed channel $\mathrm{K}|7/2, -7/2\rangle + \mathrm{Rb}|1, 0\rangle$ (refs 6,7). Here, F denotes the total atomic spin and m_F is the spin projection along the magnetic-field direction.

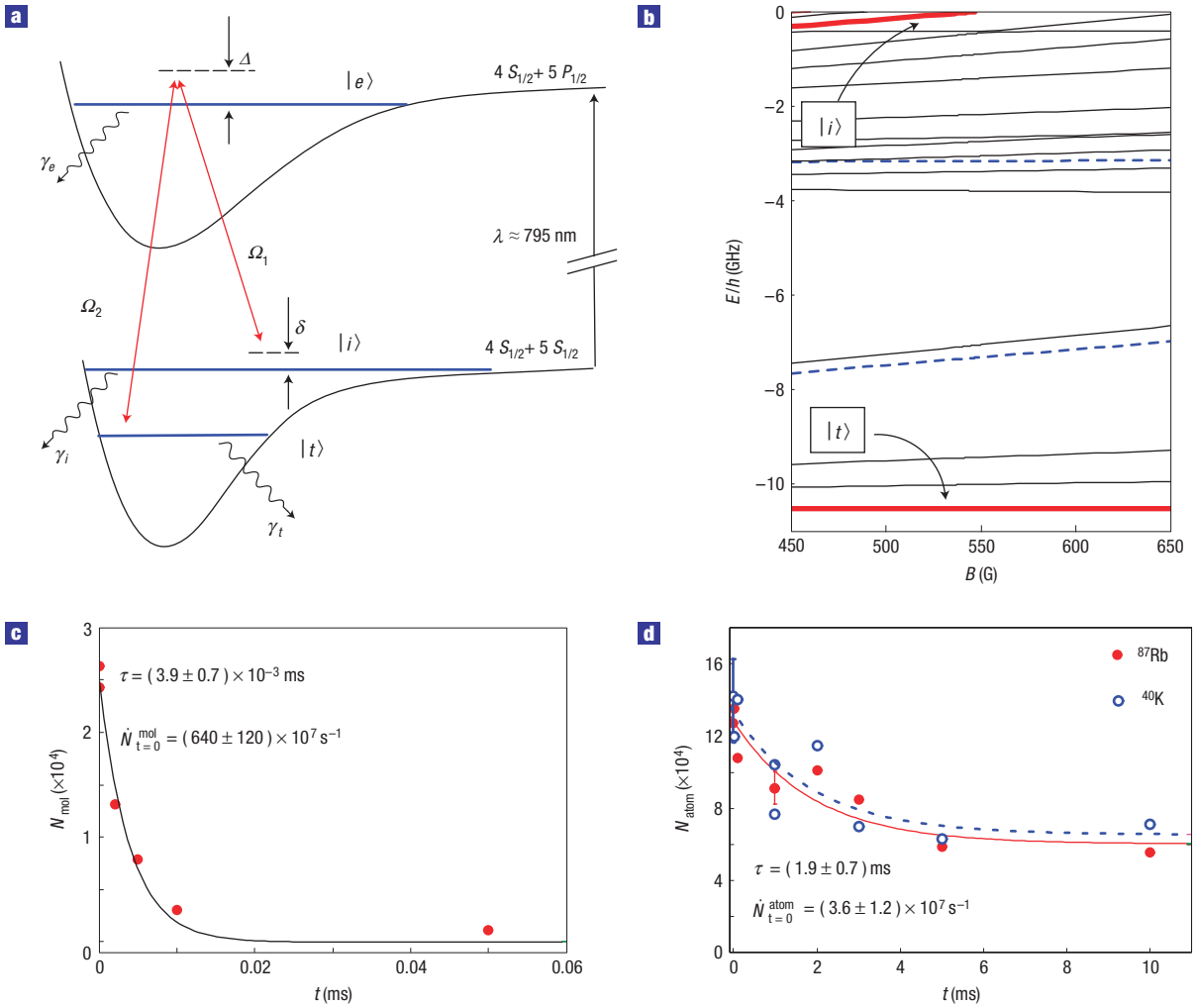

Figure 1 Schematic diagram of the STIRAP scheme. a, Schematic diagram of molecular potentials and molecular vibrational levels involved in the coherent two-photon transfer scheme. The phase-coherent lasers 1 and 2 couple the initial state $|i\rangle$ and the target state $|t\rangle$ to the intermediate state $|e\rangle$ in the excited-state molecular potential connecting to the $4S_{1/2}+5P_{1/2}$ threshold. Ω_1 and Ω_2 denote the corresponding Rabi frequencies. δ and Δ are the two-photon and single-photon detuning, respectively. γ_x represents the decay rate of state x. **b**, Calculated molecular energy structure of the $^{40}K^{87}Rb$ molecule in the ground-state molecular potential below the $K|9/2,-9/2\rangle$ $Rb|1,1\rangle$ atomic threshold. All levels have total spin-projection quantum number $M_F=-7/2$. The initial Feshbach state $|i\rangle$ and the target state $|t\rangle$ are highlighted by the red bold lines. The states observed in dark-resonance spectroscopy (see the text) are plotted with dashed blue lines. **c**,**d**, Comparison of single-photon excitation rates for the $|i\rangle \rightarrow |e\rangle$ transition, starting from Feshbach molecules (**c**) as compared with photoassociation rates from free atoms (**d**). The excitation rates are determined by measuring loss of population in state $|i\rangle$ from the trap in each case. For this set of data, $|e\rangle$ is a level in the 2(1) $v=-9$ hyperfine manifold. In **d**, the Rb (K) atom number is plotted with the red filled (open blue) circles. The red solid and blue dashed lines are simultaneous fits to the decaying Rb and K atom numbers. We assume that the loss rate ($\dot{N}_{atom}$) is the same for both components at any time. These data demonstrate that the strength of the $|i\rangle \rightarrow |e\rangle$ transition (the first leg of the STIRAP process) is markedly enhanced by starting from Feshbach molecules. With an initial molecule density of $n_{molecules} \approx 5\times10^{11}$ cm^{-3} and initial atomic densities of $n_{atoms} \approx 10^{13}$ cm^{-3}, we observe an enhancement in the initial loss rate of $\dot{N}_{molecules}/\dot{N}_{atoms} = (180\pm60)$ at a magnetic field close to the Feshbach resonance ($B=546.88$ G) (refs 28,29).

The Feshbach molecules are manipulated with light derived from a phase-coherent Raman laser system. A Ti:sapphire laser is offset-locked to a temperature-stabilized Fabry–Perot cavity, resulting in a linewidth of <20 kHz and absolute long-term frequency stability better than 2 MHz. The second laser beam is derived from an external cavity diode laser phase-locked to the Ti:sapphire laser. The two beams are π-polarized with respect to the magnetic field and propagate collinearly when irradiated onto the molecular ensemble.

In the first step, we carry out one-photon, bound–bound spectroscopy of the electronically excited $^{40}K^{87}Rb^*$ 2(1) and $2(0^{+/-})$ molecular potentials for energies within $h\times400$ GHz below the $4S_{1/2}+5P_{1/2}$ threshold. Starting from the Feshbach molecules at $B=545.88$ G, laser 1 is used to couple the molecules to vibrational levels in the excited-state molecular potentials. These electronically excited molecules subsequently decay into a multitude of molecular and atomic states where they are invisible to our detection method. Using loss spectra, we identify vibrational series of different excited-state molecular potentials, which will be reported elsewhere. After an extensive search, we have chosen the $2(0^+)$ $v=-14$ state as an intermediate coupling state $|e\rangle$. Here, v denotes the vibrational quantum number as counted from the $4S_{1/2}+5P_{1/2}$ threshold. This state is located 213 GHz below the $4S_{1/2}+5P_{1/2}$ threshold. Comparing one-photon loss rates

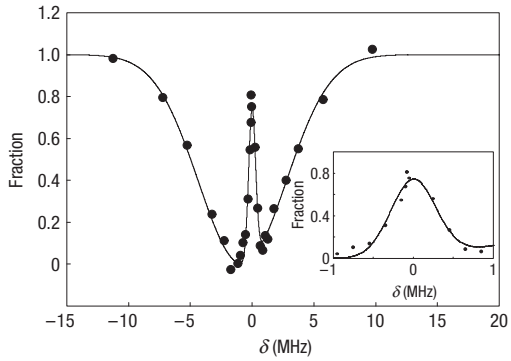

Figure 2 Dark resonance in the molecular system. In this case, the target state $|t\rangle$ is the K$|7/2,-7/2\rangle$+Rb$|1,0\rangle$ $v=-3$ state and the intermediate state $|e\rangle$ is a state in the 2(1) $v=-12$ hyperfine manifold. We shine a 10 μs square pulse of Raman light onto the Feshbach molecules and the remaining fraction of Feshbach molecules is detected. For $\delta=0$, the loss of Feshbach molecules is strongly suppressed owing to the emergence of a dark state. For this particular set of data, $\Delta\approx-2\pi\times0.8$ MHz. The inset shows the central dark-resonance feature.

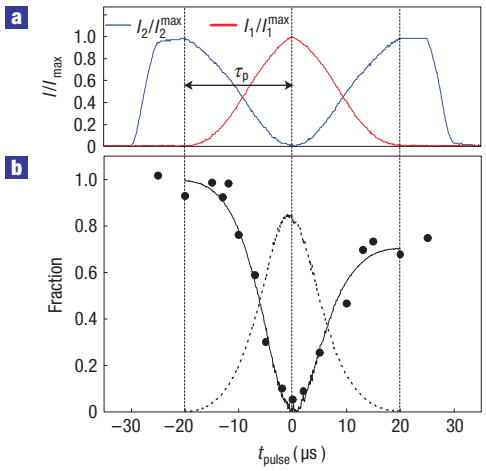

Figure 3 Time evolution of the coherent two-photon transfer. a, Counterintuitive STIRAP pulse sequence. **b**, Measured population (black circles) in the initial Feshbach state $|i\rangle$ during the STIRAP pulse sequence. To measure the population in the Feshbach state $|i\rangle$ at various times t_{pulse}, the phase coherent light fields 1 and 2 are switched off simultaneously and the Feshbach molecules are subsequently imaged by resonant absorption imaging (see the Methods section). Starting with population of 1 in $|i\rangle$, the Feshbach molecules are coherently transferred to the target state $|t\rangle$ by the first pulse sequence ($t=-\tau_p$ to $t=0$). In the deeply bound target state, the molecules are invisible to the detection light. Reversing the pulse sequence, the molecules are transferred back to the initial state $|i\rangle$ ($t=0$ to $t=\tau_p$). The solid line is a fit to the experimental data on the basis of equation (1). With $\gamma_e=2\pi\times5.7$ MHz and $\gamma_i=2\pi\times97$ Hz, we obtain $\Omega_2^{max}/\Omega_1^{max}=1.7$ and $\gamma_t=2\pi\times3$ kHz. Note that the thus-determined lifetime of the target state of $\tau_t=1/(2\pi\gamma_t)\approx330$ μs is shorter than the measured lifetime of 850 μs (Fig. 5) in the absence of light fields. The extra loss is presumably due to residual population of the lossy excited state during the STIRAP process. The dashed line is the corresponding calculated population of the target-state population during the process.

starting from Feshbach molecules with photoassociation rates of free atoms, we observe an enhancement in the excitation rate by (180 ± 60) (Fig. 1c,d).

An essential prerequisite for STIRAP is precise knowledge of possible target states. Whereas a theoretical model of the electronic ground-state potential has recently been published by Pashov *et al.*[25], the ground-state level structure of ^{40}K^{87}Rb in the near-threshold regime has never been probed experimentally. Using two-photon dark-resonance spectroscopy[26], we probe the binding energy of vibrational levels in the K$|9/2,-9/2\rangle$+Rb$|1,1\rangle$ and K$|7/2,-7/2\rangle$+Rb$|1,0\rangle$ channels at $B=545.88$ G. We probe levels with binding energies less than $h\times10.5$ GHz, which is accessible to our phase-locked laser system. Figure 2 shows a typical dark-resonance spectrum when scanning the frequency difference (δ) of the two phase-coherent laser fields in the vicinity of the frequency splitting between the two molecular ground-state levels. The presence of the near-resonant laser 2 dresses the transition $|t\rangle\rightarrow|e\rangle$ (Fig. 1), leading to destructive interference for the absorption probability of laser 1 on the probe transition $|i\rangle\rightarrow|e\rangle$ for $\delta=0$. We observe one-photon loss of Feshbach molecules with a width of ~6 MHz and a narrow dark-resonance feature in the vicinity of $\delta=0$. At $B=(545.88\pm0.05)$ G, we measure a binding energy of $h\times3.1504(10)$ GHz and $h\times10.49238(15)$ GHz for the K$|9/2,-9/2\rangle$+Rb$|1,1\rangle$ $v=-2$ and -3 states, respectively. For K$|7/2,-7/2\rangle$+Rb$|1,0\rangle$ $v=-3$, we find $h\times7.31452(15)$ GHz. The measured binding energies deviate by less than 0.1% from the theoretical prediction based on the potentials by Pashov *et al.*[25].

With possible target states and coupling states precisely determined, we use STIRAP to transfer the molecules coherently into the 10.49238 GHz bound vibrational level of the ground-state molecular potential. STIRAP is known to be a robust coherent transfer scheme in a three-level system. When two-photon resonance ($\delta=0$) is maintained, the molecules are transferred between $|i\rangle$ and $|t\rangle$ with negligible population in the lossy excited state $|e\rangle$ throughout the process. Figure 3a shows the counterintuitive STIRAP pulse sequence used in the experiment. In the first step, laser 2 is turned on, coupling the target state $|t\rangle$ to the intermediate state $|e\rangle$. While the intensity of laser 2 is ramped down from I_2^{max} to 0 within $\tau_p=20$ μs, the intensity of laser 1 is ramped up to its maximum value I_1^{max}, thereby adiabatically transferring the population from the Feshbach state into the deeply bound target state $|t\rangle$. Reversing the pulse sequence reverses the process and the transfer occurs from the deeply bound level $|t\rangle$ to the initial state $|i\rangle$, as shown for $t_{pulse}>0$ in Fig. 3a.

Figure 3b shows the time dependence of the measured population of the initial Feshbach state $|i\rangle$ during the pulse sequence. Molecules in the Feshbach state can be detected by direct high-field resonant absorption imaging, whereas molecular population in the target state is invisible to the light. During the pulse sequence, we observe the hiding of the molecules in the more deeply bound vibrational level and the transfer back into the initial state after reversal of the pulse sequence. We observe an efficiency of the double STIRAP sequence of 71%, corresponding to an efficiency of 84% for a single pulse. The transfer process can be described by an open three-level system in the rotating-wave approximation:

$$i\cdot\begin{pmatrix}\dot{\Psi}_i(t)\\ \dot{\Psi}_e(t)\\ \dot{\Psi}_t(t)\end{pmatrix}=\begin{pmatrix}\delta-i\gamma_i/2 & \Omega_1(t)/2 & 0\\ \Omega_1(t)/2 & \Delta-i\gamma_e/2 & \Omega_2(t)/2\\ 0 & \Omega_2(t)/2 & -i\gamma_t/2\end{pmatrix}\times\begin{pmatrix}\Psi_i(t)\\ \Psi_e(t)\\ \Psi_t(t)\end{pmatrix}. \quad (1)$$

Here, $|\langle\Psi_x(t)|\Psi_x(t)\rangle|^2$ and γ_x are the population and decay rate of state x, respectively (Fig. 1). The time dependence of the

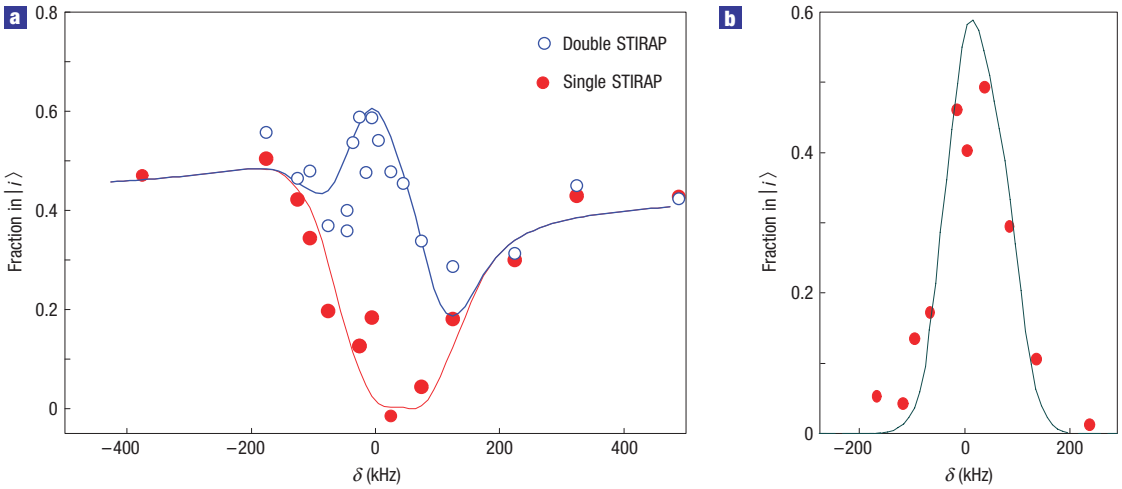

Figure 4 STIRAP line shape. **a**, STIRAP line shape for $\Delta = -2\pi \times 50$ MHz, $\Omega_1 = 2\pi \times 3.6$ MHz and $\Omega_2/\Omega_1 = 1.7$ both for single STIRAP (transfer from $|i\rangle$ to $|t\rangle$) and double STIRAP (transfer from $|i\rangle$ to $|t\rangle$ and back). The asymmetry in the line shape is due to the finite single-photon detuning Δ (see Fig. 1). **b**, Difference between the double and single STIRAP signal as plotted in **a**. The difference corresponds to the fraction of Feshbach molecules transferred into the deeply bound state and back at a given δ.

Table 1 Basic properties of KRb molecules in different vibrational levels of the ground-state molecular potential. Comparison of the binding energy, internuclear distance ('size') and dipole moment of the Feshbach molecules, the current target state K|9/2, −9/2⟩ + Rb|1, 1⟩ $v = -3$ and the absolute ground state $X^1\Sigma^+(v = -99)$ in the singlet potential[30]. The current target state has 92.5% triplet character and is therefore denoted by $a^3\Sigma^+(v = -3)$. v is the vibrational quantum number as counted from the threshold, with the least bound level labelled as $v = 0$.

Molecular property	Feshbach molecule	$a^3\Sigma^+(v=-3)$	$X^1\Sigma^+(v=-99)$
Binding energy (GHz)	0.00027	10.49238	≈125,000
Internuclear distance (a_0)	270	34	7.7
Dipole moment (ea_0)	2×10^{-11}	4.1×10^{-5}	0.3

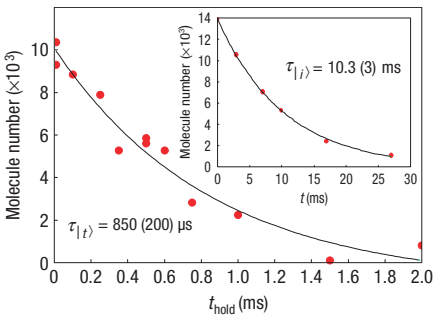

Figure 5 Lifetime of the $v = -3$ molecules. We observe a lifetime of 850 μs. The inset shows the decay of the initial Feshbach molecules, which have a lifetime of 10.3 ms.

transfer is determined by the exact pulse shape and the ratio of the maximum Rabi frequencies Ω_1^{max} and Ω_2^{max}. Given the pulse shape shown in Fig. 1a, we can extract the Rabi frequency ratio used in the experiment. Given $I_2^{max}/I_1^{max} = 0.27$, we obtain $\Omega_2^{max}/\Omega_1^{max} = (1.7 \pm 0.1)$, corresponding to a ratio of the effective transition dipole moments of (3.3 ± 0.3).

The absolute coupling strengths can be extracted from an analysis of the STIRAP efficiency as a function of the two-photon detuning δ, as shown in Fig. 4. We have measured the line shape both for a single STIRAP process ($|i\rangle \rightarrow |t\rangle$) and for a double STIRAP ($|i\rangle \rightarrow |t\rangle \rightarrow |i\rangle$). A comparison between a simulation based on equation (1) with $\Omega_2/\Omega_1 = 1.7 \pm 0.1$ and $\Delta = -2\pi \times (50 \pm 5)$ MHz and the experimental single STIRAP line-shape data yields $\Omega_1^{max} = 2\pi \times (3.6 \pm 0.5)$ MHz and $\Omega_2^{max} = 2\pi \times (6.1 \pm 0.9)$ MHz at $I_1^{max} = (3.7 \pm 1.5)\,W\,cm^{-2}$ and $I_2^{max}(1.0 \pm 0.4)\,W\,cm^{-2}$. This translates into effective transition dipole moments of $d_1^{eff} = (0.050 \pm 0.015)\,ea_0$ and $d_2^{eff} = (0.17 \pm 0.04)\,ea_0$.

Finally, we have measured the lifetime of the deeply bound molecules in the target state. Starting from the molecules in state $|i\rangle$, we apply a single STIRAP pulse to transfer the molecules into the target state $|t\rangle$. The deeply bound molecules are held in the optical dipole trap for varying times t_{hold}. A second STIRAP pulse then transfers the molecules back to the initial state, where they can be detected by high-field resonant absorption imaging. Figure 5 shows the decay of the deeply bound molecules. We observe a lifetime of the molecules in $|t\rangle$ of (850 ± 200) μs as compared with a lifetime of the initial state of (10.3 ± 0.3) ms. We observe that the lifetime of both Feshbach molecules and deeply bound molecules decreases with increasing atom density. This suggests that atom–molecule collisions limit the molecule lifetime.

In summary, we have demonstrated coherent optical transfer of heteronuclear Feshbach molecules into a 10 GHz bound vibrational level of the ground-state molecular potential. Our experiments show that the binding energy of the molecules can be significantly enhanced in a single STIRAP step. Given promising Franck–Condon factors through a number of intermediate states[9,10], the presented techniques can be extended to binding energies $\gg h \times 10$ GHz by referencing both lasers to a frequency comb bridging almost arbitrary frequency gaps[27]. The production of a polar molecular quantum gas by means of coherent optical transfer of heteronuclear Feshbach molecules might hence come within experimental reach.

METHODS

FESHBACH MOLECULE FORMATION

After evaporation of ^{40}K and ^{87}Rb in an Ioffe–Pritchard magnetic trap, 5×10^6 ^{87}Rb and 1×10^6 ^{40}K atoms are loaded into a single-beam optical dipole trap operating at 1,064 nm. At this stage, the temperature of the atoms is about 3 μK. In the optical trap, radiofrequency adiabatic rapid passage is used to prepare a $^{40}\mathrm{K}|9/2,-9/2\rangle$ and $^{87}\mathrm{Rb}|1,1\rangle$ spin mixture. It is in this combination of Zeeman states that the Feshbach resonance at a magnetic field of 546.7 G occurs between K and Rb. After ramping the magnetic field to 555 G, we further evaporate the mixture in the optical dipole trap to a temperature of $T/T_c\approx1$. Here, T_c is the critical temperature for the onset of Bose–Einstein condensation of the Rb cloud. Starting from the near-degenerate mixture of 1×10^5 ^{40}K atoms and 3×10^5 ^{87}Rb atoms, we finally use a magnetic-field ramp across the 546.7 G Feshbach resonance to couple the open scattering channel to the bound molecular state, thereby associating about 2×10^4 heteronuclear Feshbach molecules. The molecules have a temperature of 300 nK and a density of $\approx5\times10^{11}$ cm^{-3}. To suppress inelastic collisions of the molecules with remaining unbound atoms, we remove about 95% of the left-over atoms.

DIRECT RESONANT ABSORPTION IMAGING OF HETERONUCLEAR FESHBACH MOLECULES

The weakly bound heteronuclear Feshbach molecules (binding energy of 270 kHz) are detected by direct absorption imaging. The imaging uses light resonant with a cycling transition starting from the $^{40}\mathrm{K}|9/2,-9/2\rangle$ state. For small binding energies of the heteronuclear molecules, the atomic cycling transition of ^{40}K is detuned by only a few megahertz from the molecular transition. Light resonant with the atomic transition will therefore dissociate the molecules and then scatter on the resulting K atoms. To distinguish the absorption signal of weakly bound Feshbach molecules from unbound ^{40}K atoms, we flip the spin of residual $^{40}\mathrm{K}|9/2,-9/2\rangle$ atoms with a radiofrequency π-pulse on the atomic $|9/2,-9/2\rangle\rightarrow|9/2,-7/2\rangle$ transition before imaging. Note that direct imaging of molecules at high magnetic field is favourable for heteronuclear Feshbach molecules. In the heteronuclear case, both the ground and the excited electronic potentials share a $1/R^6$ dependence. The difference in energy between these two states therefore varies more slowly with the internuclear separation than in the homonuclear case, where the excited-state long-range potential varies as $1/R^3$.

Received 8 February 2008; accepted 12 May 2008; published 22 June 2008.

References

1. Santos, L., Shlyapnikov, G. V., Zoller, P. & Lewenstein, M. Bose–Einstein condensation in trapped dipolar gases. *Phys. Rev. Lett.* **85**, 1791–1794 (2000).
2. DeMille, D. Quantum computation with trapped polar molecules. *Phys. Rev. Lett.* **88**, 067901 (2002).
3. Sandars, P. G. H. Measurability of the proton electric dipole moment. *Phys. Rev. Lett.* **19**, 1396–1398 (1967).
4. Kozlov, M. G. & Labzowsky, L. N. Parity violation effects in diatomics. *J. Phys. B* **28**, 1933–1961 (1995).
5. Hudson, E. R., Lewandowski, H. J., Sawyer, B. C. & Ye, J. Cold molecule spectroscopy for constraining the evolution of the fine structure constant. *Phys. Rev. Lett.* **96**, 143004 (2006).
6. Zirbel, J. J. *et al.* Collisional stability of fermionic Feshbach molecules. *Phys. Rev. Lett.* **100**, 143201 (2008).
7. Zirbel, J. J. *et al.* Heteronuclear molecules in an optical dipole trap. Preprint at <http://arxiv.org/abs/0712.3889> (2007).
8. Kohler, T., Goral, K. & Julienne, P. S. Production of cold molecules via magnetically tunable Feshbach resonances. *Rev. Mod. Phys.* **78**, 1311 (2006).
9. Sage, J. M., Sainis, S., Bergeman, T. & DeMille, D. Optical production of ultracold polar molecules. *Phys. Rev. Lett.* **94**, 203001 (2005).
10. Stwalley, W. C. Efficient conversion of ultracold Feshbach-resonance-related polar molecules into ground state ($X^1\Sigma^+ v=0, J=0$) molecules. *Eur. Phys. J. D* **31**, 221–225 (2004).
11. Weinstein, J. D., deCarvalho, R., Guillet, T., Friedrich, B. & Doyle, J. M. Magnetic trapping of calcium monohydride molecules at millikelvin temperatures. *Nature* **395**, 148–150 (1998).
12. Bethlem, H. L., Berden, G. & Meijer, G. Decelerating neutral dipolar molecules. *Phys. Rev. Lett.* **83**, 1558–1561 (1999).
13. Sawyer, B. C. *et al.* Magnetoelectrostatic trapping of ground state OH molecules. *Phys. Rev. Lett.* **98**, 253002 (2007).
14. Rangwala, S. A., Junglen, T., Rieger, T., Pinkse, P. W. & Rempe, G. Continuous source of translationally cold dipolar molecules. *Phys. Rev. A* **67**, 043406 (2003).
15. Jones, K. M., Tiesinga, E., Lett, P. D. & Julienne, P. S. Ultracold photoassociation spectroscopy: Long-range molecules and atomic scattering. *Rev. Mod. Phys.* **78**, 483–535 (2006).
16. Wang, D. *et al.* Photoassociative production and trapping of ultracold KRb molecules. *Phys. Rev. Lett.* **93**, 243005 (2004).
17. Wynar, R., Freeland, R. S., Han, D. J., Ryu, C. & Heinzen, D. J. Molecules in a Bose–Einstein condensate. *Science* **287**, 1016–1019 (2000).
18. Thalhammer, G., Theis, M., Winkler, K., Grimm, R. & Hecker Denschlag, J. Inducing an optical Feshbach resonance via stimulated Raman coupling. *Phys. Rev. A* **71**, 033403 (2005).
19. Ospelkaus, C. *et al.* Ultracold heteronuclear molecules in a 3D optical lattice. *Phys. Rev. Lett.* **97**, 120402 (2006).
20. Papp, S. B. & Wieman, C. E. Observation of heteronuclear Feshbach molecules from a ^{85}Rb^{87}Rb gas. *Phys. Rev. Lett.* **97**, 180404 (2006).
21. Pe'er, A., Shapiro, E. A., Stowe, M. C., Shapiro, M. & Ye, J. Precise control of molecular dynamics with a femtosecond frequency comb. *Phys. Rev. Lett.* **98**, 113004 (2007).
22. Winkler, K. *et al.* Coherent optical transfer of Feshbach molecules to a lower vibrational state. *Phys. Rev. Lett.* **98**, 043201 (2007).
23. Lang, F. *et al.* Cruising through molecular bound-state manifolds with radiofrequency. *Nature Phys.* **4**, 223–226 (2008).
24. Bergmann, K., Theuer, H. & Shore, B. W. Coherent population transfer among quantum states of atoms and molecules. *Rev. Mod. Phys.* **70**, 1003–1025 (1998).
25. Pashov, A. *et al.* Coupling of the $X^1\Sigma^+$ and $a^3\Sigma^+$ states of KRb. *Phys. Rev. A* **76**, 022511 (2007).
26. Arimondo, E. & Orriols, G. Nonabsorbing atomic coherences by coherent two-photon transitions in a three-level optical pumping. *Lett. Nuovo Cimento* **17**, 333–338 (1976).
27. Cundiff, S. T. & Ye, J. Colloquium: Femtosecond optical frequency combs. *Rev. Mod. Phys.* **75**, 325–342 (2003).
28. Courteille, Ph., Freeland, R. S., Heinzen, D. J., van Abeelen, F. A. & Verhaar, B. J. Observation of a Feshbach resonance in cold atom scattering. *Phys. Rev. Lett.* **81**, 69–72 (1998).
29. Laburthe Tolra, B. *et al.* Controlling the formation of cold molecules via a Feshbach resonance. *Europhys. Lett.* **64**, 171–177 (2003).
30. Kotochigova, S., Julienne, P. S. & Tiesinga, E. Ab initio calculation of the KRb dipole moments. *Phys. Rev. A* **68**, 022501 (2003).

Acknowledgements

We acknowledge financial support from NIST, NSF and DOE. K.-K.N. and B.N. acknowledge support from the NSF, S.O. from the Alexander-von-Humboldt Foundation and P.S.J. from the ONR. We thank D. Wang for stimulating discussions and C. Ospelkaus for critical reading of the manuscript.

Author information

Reprints and permission information is available online at http://npg.nature.com/reprintsandpermissions. Correspondence and requests for materials should be addressed to J.Y. or D.S.J.